View metadata, citation and similar papers at core.ac.uk

brought to you by CORE

provided by Infoscience - École polytechnique fédérale de Lausanne

Chemical Physics Letters 602 (2014) 63–67

Contents lists available at ScienceDirect

Chemical Physics Letters

journal homepage: www.elsevier.com/locate/cplett

Microwave frequency modulation to enhance Dissolution Dynamic Nuclear Polarization

Aurélien Bornet [a], Jonas Milani [a], Basile Vuichoud [a], Angel J. Perez Linde [a], Geoffrey Bodenhausen [a,b,c,d], Sami Jannin [a,e,*]

[a] Institut des Sciences et Ingénierie Chimiques, Ecole Polytechnique Fédérale de Lausanne (EPFL), Batochime, CH-1015 Lausanne, Switzerland
[b] Département de Chimie, Ecole Normale Supérieure, 24 Rue Lhomond, 75231 Paris Cedex 05, France
[c] Université Pierre-et-Marie Curie, Paris, France
[d] UMR 7203, CNRS/UPMC/ENS, Paris, France
[e] Bruker BioSpin AG, Industriestrasse 26, 8117 Fällanden, Switzerland

ARTICLE INFO

Article history:
Received 25 February 2014
In final form 9 April 2014
Available online 18 April 2014

Dedicated to To Martial Rey, as a token of appreciation.

ABSTRACT

Hyperpolarization by Dissolution Dynamic Nuclear Polarization is usually achieved by monochromatic microwave irradiation of the ESR spectrum of free radicals embedded in glasses at 1.2 K and 3.35 T. Hovav et al. (2014) have recently shown that by using frequency-modulated (rather than monochromatic) microwave irradiation one can improve DNP at 3.35 T in the temperature range 10–50 K. We show in this Letter that this is also true under Dissolution-DNP conditions at 1.2 K and 6.7 T. We demonstrate the many virtues of using frequency-modulated microwave irradiation: higher polarizations, faster build-up rates, lower radical concentrations, less paramagnetic broadening, more efficient cross-polarization, and less critical frequency adjustments.

© 2014 The Authors. Published by Elsevier B.V. This is an open access article under the CC BY-NC-ND license (http://creativecommons.org/licenses/by-nc-nd/3.0/).

1. Introduction

Hyperpolarization methods aim at enhancing the nuclear spin polarization well beyond Boltzmann equilibrium. Since the sensitivity of NMR and MRI is directly proportional to the nuclear spin polarization, it can be enhanced considerably. Dissolution Dynamic Nuclear Polarization (D-DNP) [1,2] can provide dramatic enhancements up to four or five orders of magnitude for a broad variety of molecules and nuclear spins. Many novel applications have emerged thanks to the improved sensitivity afforded by DNP, ranging from the detection of reaction intermediates in chemistry [3,4] to the real-time metabolic imaging of tumors in medicine [5]. Since its invention in 2003, D-DNP has been generally performed under similar experimental conditions. Free radicals, embedded in a glassy matrix together with the substrate or metabolite of interest, are normally irradiated with monochromatic microwaves in the vicinity of the electron spin resonance (ESR) frequency at 1.2 K and 3.35 T [6]. Depending on the offset between the microwave frequency and the center of the ESR line, the polarization of one or several nuclear spin species can either be enhanced or depleted (positive or negative DNP, leading to positive or negative spin temperatures). The effect can arise from different DNP mechanisms, namely Thermal Mixing (TM) [7,8], the Cross Effect (CE) [9–11] or the Solid Effect (SE) [12]. Most of the theory of DNP was developed in the 1960's. The recent renaissance of DNP has led to improvements of the theory which has also become more comprehensible [13–20].

While TM is best performed with a monochromatic microwave irradiation, it has been shown recently by Thurber et al. [21], Cassidy et al. [22], and most recently by Hovav et al. [23] that DNP by CE and SE can be greatly improved by using either field-modulation or frequency-modulated microwave irradiation. We show in this Letter that the same approach is also beneficial at lower temperatures $T = 1.2$ K and at a higher magnetic field $B_0 = 6.7$ T. The effect of frequency modulation is pronounced and substantial gains in polarization by factors up to $\varepsilon_{fm} > 3$ can result in absolute ^{1}H polarization levels in excess of 60%, as reported in this Letter. Another great advantage of frequency modulation is the acceleration of the DNP build-up times by factors up to $\kappa_{fm} \sim 10$. Finally the use of frequency modulation enables a reduction in the concentration of free radicals by a factor up to 2 without hindering the final DNP efficiency. Such a reduction in radical concentration results in narrower ^{1}H NMR widths and longer T_2 and $T_{1\rho}$ at 1.2 K, which in turn significantly improves the efficiency of Cross

Abbreviations: D-DNP, Dissolution Dynamic Nuclear Polarization; PA, polarizing agent.

* Corresponding author at: EPFL, Batochime BCH 1534, CH-1015 Lausanne, Switzerland. Fax: +41 21 693 98 95.
E-mail address: sami.jannin@epfl.ch (S. Jannin).

http://dx.doi.org/10.1016/j.cplett.2014.04.013
0009-2614/© 2014 The Authors. Published by Elsevier B.V.
This is an open access article under the CC BY-NC-ND license (http://creativecommons.org/licenses/by-nc-nd/3.0/).

Polarization (CP) to transfer magnetization from ^{1}H spins to low gamma nuclear spins such as ^{13}C that have long T_1's in solution, in view, for example, of metabolic imaging experiments. After direct ^{1}H DNP, which may be combined with ^{1}H → ^{13}C CP, dissolution can be performed in a standard manner, and the sample can be transferred to a liquid-state NMR spectrometer or MRI machine while retaining a large fraction of its hyperpolarization.

2. Results and discussion

All DNP experiments reported herein were performed on a home-built DNP polarizer at T = 1.2 K in a static magnetic field B_0 = 6.7 T. The polarizer was modified from its original version [24–26] to accommodate an improved NMR circuit including double resonance on both ^{1}H and ^{13}C frequencies, resonating at f = 285.23 and f = 71.73 MHz respectively. The innovative design of the DNP insert allows one to perform ^{1}H → ^{13}C CP-DNP experiments during continuous microwave irradiation [27]. When using the free radical 4-hydroxy-2,2,6,6-tetramethylpiperidine-1-oxyl (TEMPOL) as a polarizing agent, CP-DNP has shown great potential for yielding polarizations in excess of $P(^{13}C)$ >70% in a record time using a doubly tuned solenoidal NMR coil with a 50 μL volume [28,29]. The horizontal solenoidal coil can be replaced by a saddle coil with a 1 mL volume to allow vertical access for rapid dissolution of large sample volumes. Such a compromise leads to a decrease in *rf* efficiency and homogeneity, but polarizations as high as $P(^{13}C)$ = 45% could nevertheless be achieved [30]. Using TEMPOL as a polarizing agent, ^{1}H → ^{13}C CP-DNP allows one to achieve higher $P(^{13}C)$ polarizations than direct ^{13}C DNP, we shall therefore mostly focus on ^{1}H DNP in this Letter.

Proton DNP was investigated for samples (1), (2) and (3) containing 10, 25 and 50 mM TEMPOL, respectively, in a 10:40:50 (v/v/v) H_2O:D_2O:glycerol-d_8 mixture, at T = 1.2 K. Figure 1a shows the effect of microwave frequency modulation on the ^{1}H DNP build-up behavior of sample (2) for positive or negative DNP performed at the optimal monochromatic frequencies $f_{\mu w}$ = 187.85 and 188.3 GHz. For sample (2), the amplitude of the frequency modulation was set to $\Delta f_{\mu w}$ = 100 MHz with a modulation frequency f_{mod} = 10 kHz. A scheme explaining these frequency modulation parameters is presented in Figure 1b. Sinusoidal and triangular frequency modulation had identical efficiencies. According to Figure 1a, frequency modulation provides a drastic way of increasing the proton polarization $P(^1H)$, while simultaneously increasing the DNP build-up rate $R_{DNP}(^1H) = 1/\tau_{DNP}(^1H)$. Table 1 gives the final proton polarization $P(^1H)$ and the corresponding build-up rates $R_{DNP}(^1H)$ with and without frequency modulation for positive and negative DNP effects, and for three different radical concentrations. The effect of frequency modulation is hardly remarkable at a high radical concentration of 50 mM, but it is much more pronounced as the radical concentration is decreased to 25 or 10 mM.

Increasing the radical concentration enhances electron–electron dipolar couplings which enable rapid spectral spin diffusion within the broad inhomogeneous ESR line of TEMPOL. As a consequence, a larger fraction of the electron spins can contribute to the DNP process. Usually, in absence of microwave frequency modulation, the radical concentration needs to be carefully optimized. If the radical concentration is too low, only a very small fraction of electron spins will contribute to DNP, which will translate in low nuclear spin polarizations and very long build-up times. On the other hand, if the electron spin concentration is too high, the ESR line will tend to be homogeneously broadened well beyond its inhomogeneous width, which will translate into fast build-up rates, but with poor nuclear spin polarizations. In practice, the best radical concentration was found to be around 50 mM at 1.2 K and

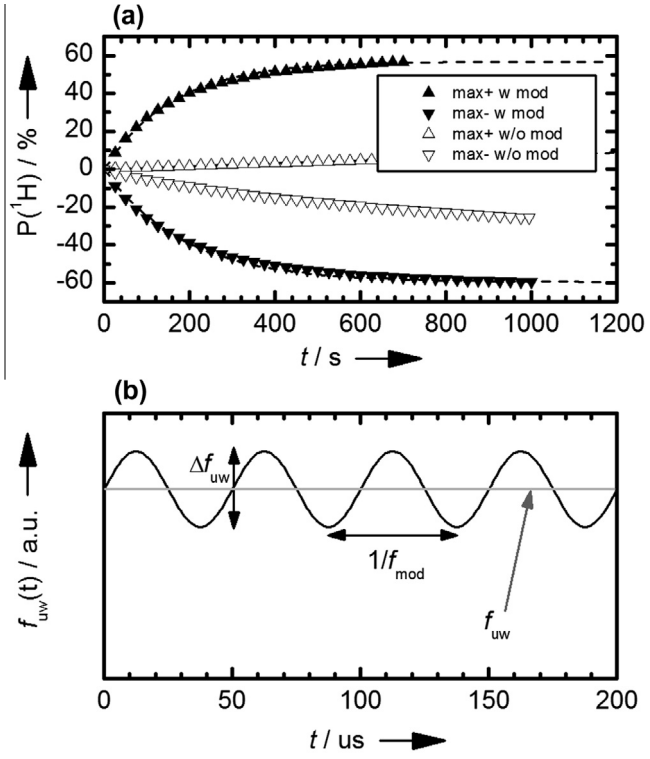

Figure 1. (Top) Negative and positive ^{1}H DNP build-up curves measured at T = 1.2 K and B_0 = 6.7 T, with and without frequency modulation, in sample 2 (a 10:40:50 (v/v/v) H_2O:D_2O:glycerol-d_8 mixture with 25 mM TEMPOL). The optimal frequencies $f_{\mu w}$ = 187.85 and 188.3 GHz were set for positive or negative DNP respectively, with a microwave power $P_{\mu w}$ = 87.5 mW. An amplitude $\Delta f_{\mu w}$ = 100 MHz was used for frequency modulation. (Bottom) Scheme illustrating the frequency modulation method. The microwave frequency typically varies in a sinusoidal fashion according to $f_{\mu w}(t) = f_{\mu w} + ½\ \Delta f_{\mu w} \sin(2\pi f_{mod}\ t)$ where $f_{\mu w}$ is the average frequency, $\Delta f_{\mu w}$ the amplitude of the frequency modulation, and f_{mod} the modulation frequency.

Table 1
Proton polarization and build-up times at T = 1.2 K and B_0 = 6.7 T for different radical concentrations in a 10:40:50 (v/v/v) H_2O:D_2O:glycerol-d_8 mixture, with and without frequency modulation.

[PA]/mM	Modulation	$P^+(^1H)$ (%)	$\tau^+_{DNP}(^1H)$ (s)	$P^-(^1H)$ (%)	$\tau^-_{DNP}(^1H)$ (s)
10	With	14.5*	2600 ± 1000**	−21.1*	2500 ± 1000**
	Without	0.9*	NA***	−1.2*	NA***
25	With	57.3	159 ± 1.8	−60.7	185 ± 2
	Without	9.3*	9000 ± 2000**	−29.5	625 ± 11
50	With	61.3	108 ± 1.6	−63.3	152.2 ± 2
	Without	21.9	338 ± 7	−43.7	218 ± 4

* DNP maximum was not reached; the polarization shown was achieved after 20 min of microwave irradiation.
** Fits have large uncertainties because only the first 20 min of the DNP build-up curve were recorded.
*** Estimates of the build-up time not available because of poor fits.

6.7 T in our laboratory [29]. When frequency modulation is used, the optimization of the electron concentration can be largely dispensed with. The fraction of the ESR line where DNP is effective is no longer related to the radical concentration. In fact, frequency modulation can play a similar role as spectral spin diffusion. A more detailed theoretical explanation supported by numerical simulations is given by Hovav et al. [23].

(Figure 2a) shows the ESR line-shape of TEMPOL measured in our DNP polarizer at T = 1.2 K and B_0 = 6.7 T by longitudinally detected ESR (LODESR) with a home-built apparatus inspired by

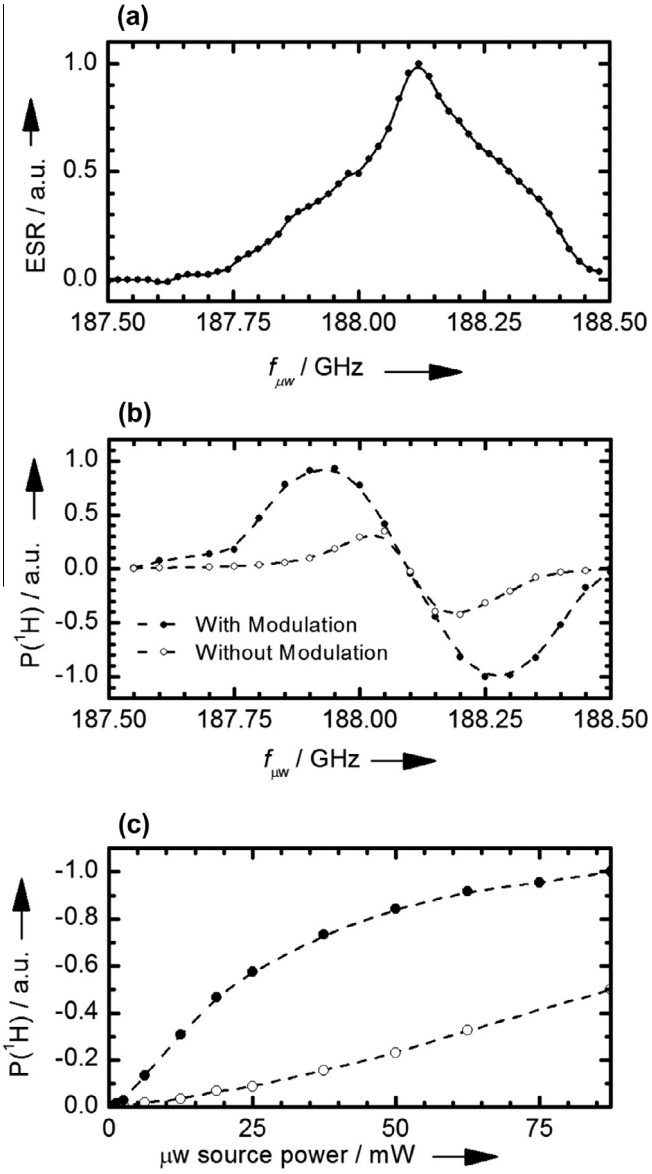

Figure 2. (a) ESR line shape of the radical TEMPOL measured in the DNP polarizer at $T = 1.2$ K and $B_0 = 6.7$ T. (b) Polarization $P(^1H)$ with and without frequency modulation ($\Delta f_{\mu w} = 100$ MHz) in sample (2) (a 10:40:50 (v/v/v) H_2O:D_2O:glycerol-d8 mixture with 25 mM TEMPOL), as a function of microwave frequency and (c) as a function of microwave power. Lines are drawn to guide the eye.

the work of Granwehr et al. [31] but adapted to our purposes. In Figure 2b, the DNP microwave spectrum measured for sample (2) shows the proton polarization $P(^1H)$ achieved with DNP as a function of the irradiation frequency $f_{\mu w}$ with and without frequency modulation. The DNP microwave spectra, measured with or without microwave frequency modulation, are contained within the limits of the ESR spectra, which suggests that the Cross Effect or Thermal Mixing are likely to be the dominant DNP mechanisms. In fact, if the Solid Effect were significant, it would allow the wings of these DNP microwave spectra to extend beyond the limits of the ESR line, typically by as much as the proton Larmor frequency. Finally, the absence of a unique spin temperature for ^1H and ^{13}C under DNP definitely supports the idea that the Cross Effect is prevailing. The line-shapes of the DNP microwave spectra are substantially different with or without microwave frequency modulation. The DNP microwave spectrum measured with frequency modulation has a separation between its positive and negative optima roughly equal to the proton Larmor frequency $f = 285.23$ MHz, which is typical for the Cross Effect. On the other hand, the DNP microwave spectrum measured without frequency modulation, in addition to showing reduced DNP performance, has a width shrunk to ca. 150 MHz. One possible explanation is that without frequency modulation, only a small fraction of the electron spins contribute to the DNP process, and this fraction become even smaller when the microwave frequency is shifted towards the tails of the ESR spectrum. As a result, DNP build-up times become increasingly longer, and DNP enhancements are reduced. Figure 2c shows the proton polarization $P(^1H)$ as a function of microwave power with and without frequency modulation. Thus, microwave frequency modulation is advantageous in terms of final polarization, required microwave power, and radical concentration.

The parameters used in this Letter were carefully optimized: modulation amplitude $\Delta f_{\mu w} = 100$ MHz and modulation frequency $f_{mod} = 10$ kHz. Figure 3 shows how $P(^1H)$ depends on $\Delta f_{\mu w}$ and f_{mod}. The most striking feature is that the optimal condition is rather flat with $20 < \Delta f_{\mu w} < 100$ MHz and $1 < f_{mod} < 1000$ kHz. As a general principle, the modulation of the frequency should cover a significant part of the ESR lineshape, resulting in a constructive DNP effect (either positive or negative), and the modulation frequency should be faster than the electron spin–lattice relaxation rate.

Microwave frequency modulation can be applied to D-DNP, either to improve direct ^1H or ^{13}C hyperpolarization, or for $^1H \rightarrow {}^{13}C$ CP. There are several advantages of using frequency modulation in this context. A decrease in radical concentration results in an extension of nuclear spin–lattice relaxation times both before and after dissolution, which of course improves the preservation of hyperpolarized magnetization. Additionally, we observed a

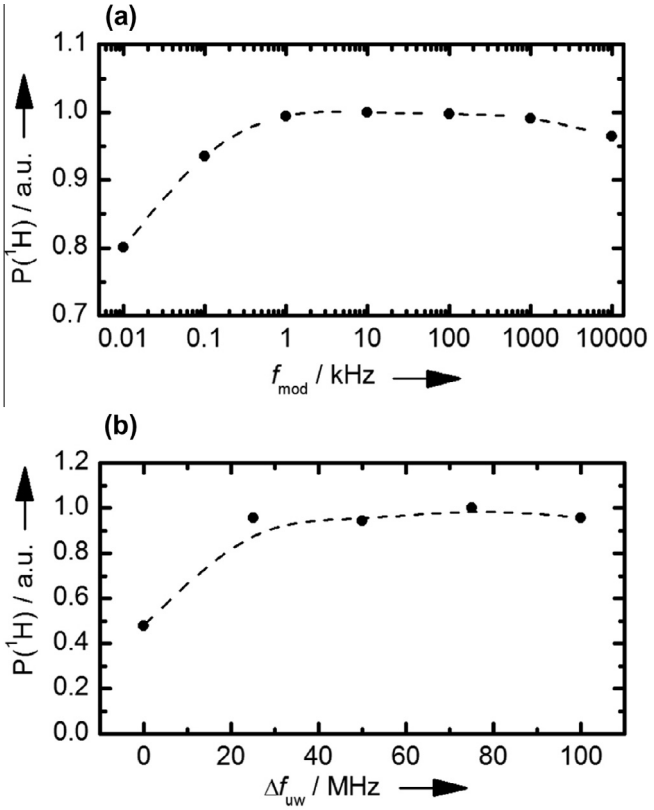

Figure 3. Proton polarization $P(^1H)$ in sample (2) (a 10:40:50 (v/v/v) H_2O:D_2O:glycerol-d8 mixture with 25 mM TEMPOL) (a) as a function of the frequency of the modulation f_{mod} (with a fixed amplitude $\Delta f_{\mu w} = 100$ MHz and power $P_{\mu w} = 87.5$ mW) and (b) as a function of the modulation amplitude $\Delta f_{\mu w}$ (with a fixed modulation frequency $f_{mod} = 10$ kHz and power $P_{\mu w} = 87.5$ mW).

significant ^{1}H line narrowing in the [1-^{13}C]acetate samples at 1.2 K owing to the reduction of paramagnetic line broadening from 35 to 25 kHz for samples (3) and (2) respectively. These positive side-effects of the reduction of the radical concentration, which are made possible by frequency modulation, make CP more efficient even with reduced radio-frequency fields. Figure 4 illustrates this concept by showing that, even though $P(^1H)$ slightly decreases when the radical concentration is reduced from 50 mM to 25 mM, $P(^{13}C)$ is significantly increased after CP. Since $P(^{13}C)$ is obtained from $P(^1H)$ by $^1H \rightarrow {}^{13}C$ CP, one would not expect such an advantage. However, the improved CP efficiency compensates for the decrease in ^{1}H polarization.

In conclusion, we have shown that microwave frequency modulation can enhance the polarization in low temperature DNP in view of dissolution experiments. The experimental implementation of such a modulation is straightforward, and the parameters can be easily optimized. The gain in polarization brought about by frequency modulation is modest for high radical concentrations when the ESR spectra are homogeneously broadened, but becomes substantial for low radical concentrations when the ESR linewidths are inhomogeneous. When the radical concentration is reduced, cross-polarization (CP) becomes more efficient. Even if techniques for the elimination of radicals exist [32–35], they are usually time consuming, and losses in polarization due to paramagnetic relaxation cannot be avoided. Enabling efficient D-DNP experiments at lower radical concentrations is of considerable interest in this respect. Obviously, the reduction of the concentration of toxic radicals is even more important for *in vivo* imaging. In this field, many groups still favor Dissolution-DNP by direct ^{13}C polarization with narrow line radicals such as trityls, and seem to hesitate to resort to $^1H \rightarrow {}^{13}C$ Cross Polarization using wide line radicals such as nitroxides. We are therefore currently extending this Letter to other radicals such as trityls, Galvinoxyl or BDPA.

3. Methods

3.1. Sample preparation

TEMPOL was dissolved in a 10:40:50 (v/v/v) H_2O:D_2O:glycerol-d_8 mixture. To verify the efficiency of $^1H \rightarrow {}^{13}C$ CP, 3 M [1-^{13}C] acetate was added to the mixture. TEMPOL and D_2O were purchased from Sigma Aldrich, [1-^{13}C]acetate from Cambridge Isotopes, and glycerol-d_8 from Cortecnet. For each sample, 10 pellets of 10 μL each (a total of 100 μL) were frozen at 70 K in liquid nitrogen, visually inspected to ensure that they remained translucent and glassy, and then transferred to the DNP polarizer at 4.2 K.

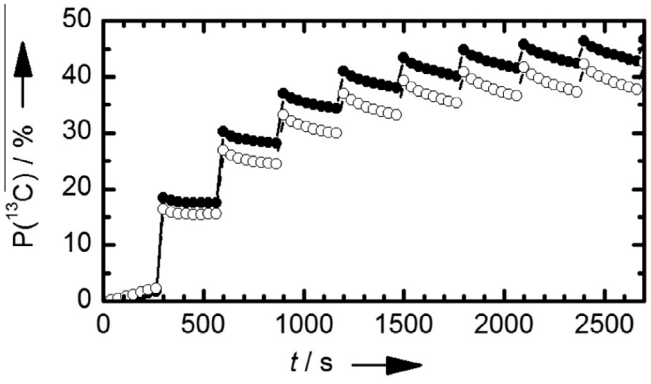

Figure 4. DNP build-up curve of the ^{13}C polarization, measured with multiple cross-polarization contacts, for 3 M [1-^{13}C]acetate doped with 25 mM TEMPOL with frequency modulation (filled circles) or with 50 mM TEMPOL without frequency modulation (empty circles) in a 10:40:50 (v/v/v) H_2O:D_2O:glycerol-d8 mixture.

3.2. NMR measurements

NMR signals were measured with a Bruker Avance 2 spectrometer. The polarization was calibrated at $T = 4.2$ K and $B_0 = 6.7$ T, where the Boltzmann polarizations without DNP are $P(^1H) = 0.00163$ and $P(^{13}C) = 0.00041$, by applying 32 pulses with 1° nutation angles for ^{1}H, and 16 pulses with 5° nutation angles for ^{13}C. The depletion of the polarization caused by these pulses, which amounts to a factor 0.999 for ^{1}H and 0.95 for ^{13}C, was taken into account. The exact same pulses were used during the measurement of DNP-enhanced spectra. Larger nutation angles were avoided to prevent receiver saturation.

3.3. Cross Polarization

$^1H \rightarrow {}^{13}C$ CP experiments were accomplished during DNP by applying radio-frequency modulated WURST pulses simultaneously to both channels, with durations optimized to 2 ms for sample (2) and 1 ms for sample (3), with frequency sweeps of 100 kHz, and amplitudes $\gamma B_1/(2\pi) = 20$ kHz on both channels to match the Hartmann–Hahn condition.

3.4. Microwave irradiation

DNP was performed by microwave irradiation at frequencies $187.5 < f_{\mu w} < 188.5$ GHz, and with a maximum power $P_{\mu w} \approx 87.5$ mW at the input of the DNP insert. Microwaves were generated with a source (Elva VCOM-10/0.5/94/400) delivering up to $P_{\mu w} \approx 400$ mW at $f_{\mu w} = 94$ GHz ± 250 MHz at the WR-10 output in the rectangular fundamental TE_{10} mode. At this stage the frequency was controlled directly by a voltage controlled oscillator unit (VCO) by a constant or modulated voltage (Stanford Research Systems DS345). The voltage source combined with the Elva VCO enables fast (up to 10 MHz) and broad frequency modulation over a range of ± 500 MHz. A doubler (Virginia Diode D200) was used to double the microwave frequency, thus providing $f_{\mu w} = 188 \pm 0.5$ GHz with $P_{\mu w} \approx 87.5$ mW at the WR-5 waveguide output in the TE_{10} mode. A commercial rectangular-to-circular transition device (Quinstar QWC series) was placed directly after the doubler to convert the rectangular TE_{10} mode to a circular TE_{11} mode. The microwave beam propagates in a 4.5 mm diameter oversized stainless steel waveguide equipped with two home-built gold-plated miter bends. The microwave beam is directed horizontally on the side of the sample.

Acknowledgements

The authors thank Martial Rey and Dr. Pascal Miéville for valuable assistance. We are indebted to Yonatan Hovav, Prof. Shimon Vega, and Prof. Daniela Goldfarb and for inspiring discussions. This work was supported by the Swiss National Science Foundation, the Ecole Polytechnique Fédérale de Lausanne (EPFL), the Swiss Commission for Technology and Innovation (CTI), Bruker BioSpin Switzerland AG, the French CNRS, and the European Research Council (ERC).

References

[1] J.H. Ardenkjaer-Larsen et al., Proc. Natl. Acad. Sci. U.S.A. 100 (18) (2003) 10158.
[2] A. Abragam, M. Goldman, Rep. Prog. Phys. 41 (3) (1978) 395.
[3] C. Hilty, S. Bowen, Org. Biomol. Chem. 8 (15) (2010) 3361.
[4] S. Bowen, G. Sekar, C. Hilty, NMR Biomed. 24 (8) (2011) 1016.
[5] S.J. Nelson et al., Sci. Trans. Med. 5 (198) (2013).
[6] J.H. Ardenkjaer-Larsen, A.M. Leach, N. Clarke, J. Urbahn, D. Anderson, T.W. Skloss, NMR Biomed. 24 (8) (2011) 927.
[7] B.N. Provotorov, Sov. Phys. JETP-USSR 14 (5) (1962) 1126.
[8] M. Goldman, A. Landesman, Phys. Rev. 132 (2) (1963) 610.

[9] A.V. Kessenikh, A.A. Manenkov, G.I. Pyatnitskii, Sov. Phys.-Solid State 6 (3) (1964) 641.
[10] C.F. Hwang, D.A. Hill, Phys. Rev. Lett. 18 (4) (1967) 110.
[11] D.S. Wollan, Phys. Rev. B 13 (9) (1976) 3671.
[12] C.D. Jeffries, Phys. Rev. 106 (1) (1957) 164.
[13] Y. Hovav, A. Feintuch, S. Vega, Phys. Chem. Chem. Phys. 15 (1) (2013) 188.
[14] Y. Hovav, O. Levinkron, A. Feintuch, S. Vega, Appl. Magn. Reson. 43 (1–2) (2012) 21.
[15] Y. Hovav, A. Feintuch, S. Vega, J. Magn. Reson. 214 (2012) 29.
[16] Y. Hovav, A. Feintuch, S. Vega, J. Magn. Reson. 207 (2) (2010) 176.
[17] S. Jannin, A. Comment, J.J. van der Klink, Appl. Magn. Reson. 43 (1–2) (2012) 59.
[18] S.C. Serra, A. Rosso, F. Tedoldi, Phys. Chem. Chem. Phys. 15 (21) (2013) 8416.
[19] S.C. Serra, A. Rosso, F. Tedoldi, Phys. Chem. Chem. Phys. 14 (38) (2012) 13299.
[20] K.N. Hu, G.T. Debelouchina, A.A. Smith, R.G. Griffin, J. Chem. Phys. 134 (12) (2011).
[21] K.R. Thurber, W.M. Yau, R. Tycko, J. Magn. Reson. 204 (2) (2010) 303.
[22] M.C. Cassidy, H.R. Chan, B.D. Ross, P.K. Bhattacharya, C.M. Marcus, Nat. Nanotechnol. 8 (5) (2013) 363.
[23] Y. Hovav, A. Feintuch, S. Vega, D. Goldfarb, J. Magn. Reson. 238 (2014) 94.
[24] A. Comment et al., Appl. Magn. Reson. 34 (3–4) (2008) 313.
[25] S. Jannin, A. Comment, F. Kurdzesau, J.A. Konter, P. Hautle, B. van den Brandt, J.J. van der Klink, J. Chem. Phys. 128 (24) (2008) 241102.
[26] A. Comment et al., Concepts Magn. Reson. B 31B (4) (2007) 255.
[27] S. Jannin, A. Bornet, S. Colombo, G. Bodenhausen, Chem. Phys. Lett. 517 (4–6) (2011) 234.
[28] S. Jannin, A. Bornet, R. Melzi, G. Bodenhausen, Chem. Phys. Lett. 549 (2012) 99.
[29] A. Bornet, R. Melzi, S. Jannin, G. Bodenhausen, Appl. Magn. Reson. 43 (1–2) (2012) 107.
[30] A. Bornet, R. Melzi, A.J.P. Linde, P. Hautle, B. van den Brandt, S. Jannin, G. Bodenhausen, J. Phys. Chem. Lett. 4 (1) (2013) 111.
[31] J. Granwehr, J. Leggett, W. Kockenberger, J. Magn. Reson. 187 (2) (2007) 266.
[32] Leach AM, Miller P, Telfeyan E, & Whitt DB (2009) Co. GE US2009263325-A1 (2009).
[33] L. Lumata et al., Rsc Adv. 2 (33) (2012) 12812.
[34] L. Lumata et al., Chem-Eur J 17 (39) (2011) 10825.
[35] T. Harris, C. Bretschneider, L. Frydman, J. Magn. Reson. 211 (1) (2011) 96.